ZnO nanowires

DOI: 10.1002/smll.200800060

Gold at the root or at the Tip of ZnO Nanowires: A Model**

Dong Sik Kim, Roland Scholz, Ulrich Gösele, and Margit Zacharias*

Semiconducting nanowires have many unique features that are required for potential applications in future electronics and optoelectronics. Nanowires with reliable functionality can be incorporated into advanced electronic devices. Much effort has been devoted to engineering nanowire properties, for example, to achieve segmented doping along a nanowire and precise controlling over interfaces within a heterostructure nanowire.[1,2] A quantitative understanding of nanowire growth is of particular importance for better control of nanowire properties. Several investigations have shown some unexpected aspects of growth behavior. For instance, the dynamic reshaping of catalyst particles during nanowire growth determines the length and shape of Si nanowires.[3,4] A self-oscillation process results in the irregular morphology of nanowires.[5] Most nanowires are grown by the vapor–liquid–solid (VLS) process, however, in some cases a solid catalytic metal particle is also assisting the condensation of material into the one-dimensional form.[6,7,8]

Compared to element[9] and III-V semiconductor nanowires[10] the growth behavior of oxide semiconductor nanowires, in particular ZnO — an important functional oxide material with a direct band gap around 3.4 eV and a high exciton binding energy of 60 meV — are not well understood. For Au catalyzed ZnO nanowire growth, Au nanoparticles were not only observed at the tip[11] of the wires, which is typical for Au catalyzed semiconductor nanowire growth, but sometimes also at the root[12] of wires after growth. Such complex and diverse nucleation and growth processes were also found in carbon nanotube formation: growth can occur either at the tip[13] or at the root[14] of the tube, and with a tube diameter that does not necessarily match that of the catalyst particle.[15]

[*] D. S. Kim, Dr. R. Scholz, Prof. U. Gösele
Max Planck Institute of Microstructure Physics
Weinberg 2, 06120 Halle (Germany)
Fax: (+49) 345-551-1223
E-mail: dskim@mpi-halle.de
Prof. M. Zacharias
Faculty of Applied Science (IMTEK), Albert-Ludwigs University Freiburg Georges-Köhler-Allee, 79110 Freiburg (Germany)

[**] This work was supported by the International Max Planck Research School for Science and Technology of Nanostructures (Nano-IMPRS) in Halle. We thank A. Dadgar and A. Krost for supplying GaN/Si substrates and N. Zakharov for useful discussions.

Supporting Information is available on the WWW under http://www.small-journal.com or from the author.

Here we compare the growth behavior of ZnO nanowires nucleated from predefined Au particles on planar substrates or on nanowire backbones in order to get a better quantitative picture of the growth mechanisms. In addition, we study the influence of the surface migration of Au atoms for the epitaxial growth of ZnO nanowires at lattice-matched substrate.

Typical morphologies of ZnO nanowires grown at the SiO_2/Si substrate and the ZnO nanowire backbones are shown in Figure 1a and b, respectively. Here we denote ZnO nanowires grown at the SiO_2/Si substrate as wires A, and ZnO nanowires grown at the ZnO nanowire backbones as wires B. All wires A were grown from the positions of Au colloid particles. In many cases, a number of wires A originated from a single position. Transmission electron microscopy (TEM) investigations reveal that the wires A with a length of several tens of micrometers are terminated by a flat plane (Figure 1c). In all cases, the nucleating Au particles remained at the root of the wires A (see for instance Figure S3 in the Supporting Information). In contrast, for wires B, all nanowire branches end with Au nanoparticles at their tips. There are two kinds of branches: the first kind lifts off from the nanowire backbone (straight branch) and the other kind grows along the surface of the wires (crawling branch) as shown in Figure 1b. Compare also the corresponding TEM images Figure 1d and e. In Figure 1f we show a TEM image of a junction at the nanowire backbone and branch. Figure Figure 1g is the magnified view of the solid line box in Figure 1f. Both, the nanowire backbone and the branch have a preferential growth direction of [0001]. A selected-area diffraction pattern from the junction is shown in Figure 1h confirming the above-mentioned growth direction of the nanowires.

The difference between wires A and B is the position of Au particles in the nanowires: the Au particles are located at the root of wires A but at the tip of wires B. Also the size distribution of the wires A is broader than that of wires B, wires A vary from 20 to 500 nm but wires B only from 50 to 100 nm. (See size-distribution plots of Figure S4 in the Supporting Information.)

In order to explain the differences in modes of growth in the experimental studies, we first concentrate on the nucleation process and then on the subsequent wire growth. We assume that single adsorbed ZnO molecules are the only species that are effectively mobile on the surface. The interactions between the adsorbed ZnO molecules and Au are schematically illustrated in Figure 2. When the nucleation process proceeds in the beginning of the growth stage, the population of adsorbed ZnO molecules changes as a result of the competition between the *arrival* of particles from the incoming flux of ZnO vapor and *loss* by evaporation and deposition on the substrate, and by diffusion capture or direct impingement on the Au particle. Because nucleation events do not take place without the presence of Au on the substrate, the only considerable *loss* is diffusive capture by the Au particles and evaporation. Note that Au atoms have a strong binding affinity to ZnO that results from the polarity of ZnO: the binding energy for Au on the polar surface of ZnO was estimated to be 0.94 eV.[16] In spite of the relatively large misfit of 11%, Au films grow epitaxially on ZnO substrates even at low temperature.[17]

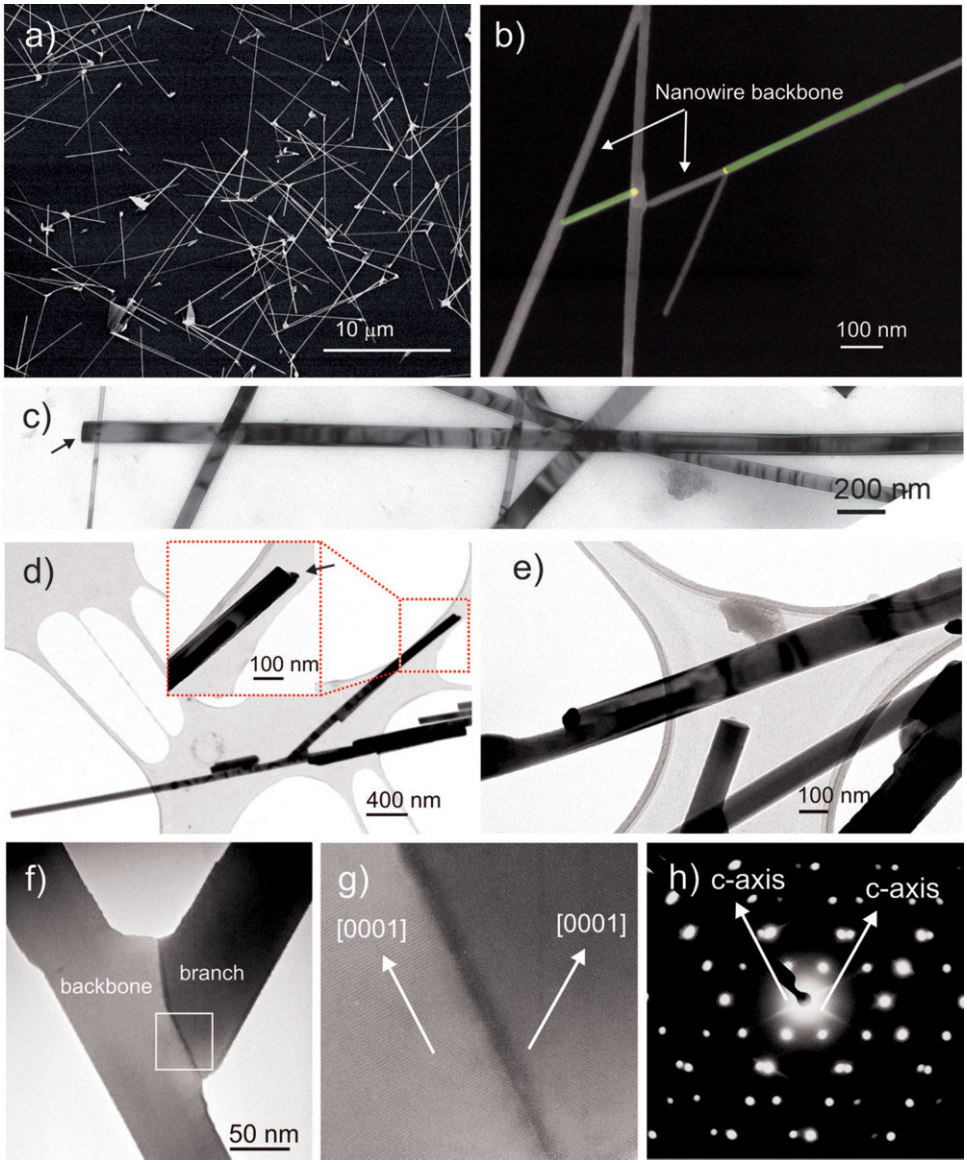

Figure 1. Scanning electron microscopy (SEM) and TEM images of ZnO nanowires grown at SiO_2/Si substrate and nanowire backbones. a) SEM image of wires A. b) SEM image of wires B. Nanowires branches and Au particles in the image are colored in light green and light yellow, respectively. For an original image see Figure S2 in the Supporting Information. c) TEM image of wire A. An arrow indicates the tip of the nanowire. d) TEM image of straight branch. Inset shows a high-magnification image from the tip of wire (dotted line box). An arrow indicates an Au particle. e) TEM image of a crawling branch. f) TEM image at the junction of wire B. g) High-magnification image of junction (solid line box) in Figure 1f. The lattice of a ZnO nanowire backbone and branch is visible and show their growth direction of [0001]. h) Selected-area electron-diffraction pattern recorded from the junction.

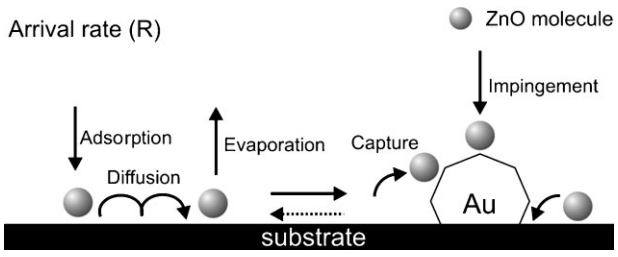

Figure 2. Schematic illustration of nucleation process with the presence of Au particle: ZnO adsorption, evaporation, diffusion, and capture by Au. The arrival rate (*R*) is the experimental variable. The dotted line indicates the process that is less important in this growth mode.

In the regime of the diffusion-induced nanowire growth, the surface of Au particles at the SiO_2/Si substrate become saturated with ZnO during the nucleation process as result of supersaturation, diffusion of adsorbed ZnO molecules, and their affinity to Au. Once Au particles are saturated by ZnO then molecules from the ZnO vapor contribute to the formation of ZnO nuclei since ZnO has unique self-assembly characteristics. ZnO has a tetrahedral fundamental unit cell in which the Zn ions are surrounded tetrahedrally by O ions and vice versa that results from the sp^3 hybridized orbital. Because the normal direction to each plane of the tetrahedron is parallel to the c-axis, ZnO has a preferential orientation toward the c-axis. Accordingly, we found that both 20 and 80 nm Au particles resulted in a similar size distribution

because the size of wires were not dependent on that of the Au particles but is determined by the size of the ZnO nuclei.

Let us now discuss the case of nucleation at Au particles deposited on already existing ZnO nanowires. In this case the only valid pathways for the ZnO molecules are the direct impingement upon the Au particles and the surface diffusion along the pre-existing ZnO nanowire towards the Au particles. Because of the limited supply, the active area of Au particles does not become saturated by ZnO but acts as a preferential adsorption site and promotes the delivery of ZnO molecules to the Au–ZnO nanowire interface. The reduced flux of molecules drives the energetically more favorable epitaxial growth of ZnO layers at the Au–substrate interface with a higher rate (e.g., nucleation rate) than the saturation rate at the surface of the Au particles. Thus wires B grow while keeping the Au particles at the growth front. In Figure 3 the basic steps of the growth modes of wires A and B are shown schematically. In addition, the fluxes of ZnO molecules contributing to the growth of wires A and B are roughly estimated to be about 1.8×10^7 and 2.4×10^6 molecules $\mu m^{-2} \cdot min^{-1}$, respectively, based on the wire volume per unit area. We assume that all incoming vapor was incorporated into the wires either by diffusion or direct impingement without any loss by evaporation.

It is not clear whether Zn or ZnO vapor dominantly contributes to the anisotropic crystal growth in the presence of Au particles.[18] If Zn atoms are considered to be the main species, then Au particles should alloy with Zn and ZnO nanowires should grow with the assistance of liquid catalytic particles, so that the nanowire diameter is determined by the size of the Au particles. The mechanism involved in this catalytic growth is generally referred to as the vapor–liquid–solid (VLS) process.[19] However, the observed growth behavior of ZnO nanowires does not fit the VLS mechanism. The diameter of the nanowires is larger than that of the Au particles as shown in Figure 4. Furthermore, X-ray diffraction (XRD) analyses reveal that the Au particles are solid during ZnO nanowire growth.[20]

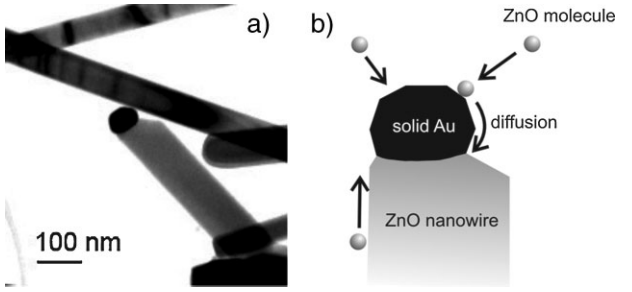

Figure 4. a) TEM image of wire B near tip. b) Schematic illustration of a possible growth mechanism. ZnO vapor sticks to solid Au particle followed by diffusion along the surface and builds up ZnO lattice. Alternatively adatoms of ZnO diffuse along the wire surface and incorporate into growth front.

If ZnO molecules are taken as major vapor-phase constituents, the growth picture of wires B with the assistance of Au particles becomes apparent. It was demonstrated that the metallic Au phase is clearly isolated from the ZnO matrix when the annealing temperature is increased.[21] Also the size of Au particles used in the growth experiments was 50 nm, which excludes a possible liquid phase of Au particles from a size effect.[22] Based on the experimental observations we suggest the growth process illustrated in Figure 4b. ZnO/C source material produces Zn vapor after a carbothermal reduction reaction. During the transportation to the Au particles, the Zn vapor is oxidized by reaction with carbon monoxide and arrives in the form of ZnO molecules.[23] ZnO molecules are incorporated into the growth front by diffusion along the nanowire surface or direct impingement on a Au particle. Therefore, the growth mechanism is slightly different from a typical vapor–solid–solid (VSS) process. From this point of view, the growth mode of ZnO nanowires has different characteristics compared to elemental or III–V semiconductors. With respect to the Au particles that assisted wire growth, initially spherical Au particles become approximately hemispherical and their volume decreases during wire growth. For instance, an Au particle with the volume of 7.4×10^4 nm^3 was reduced to 5.6×10^4 nm^3 after growth. Some Au atoms might have evaporated or migrated along the wires into the substrate.[27]

Epitaxial nanowire growth is required for optical studies and device applications such as vertical-surround-gate field-effect transistors. Similar growth condition to

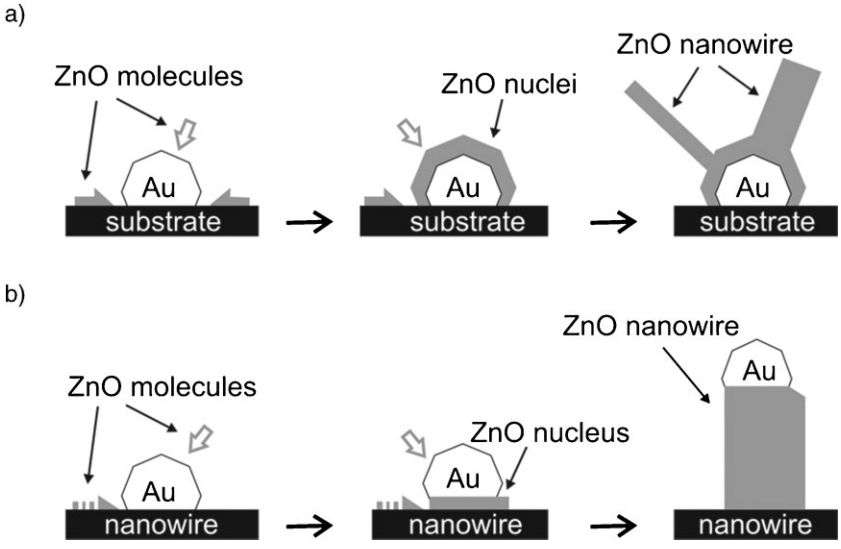

Figure 3. Schematic representation of the basic steps of the growth modes of wires A and B. a) High diffusion flux of adsorbed ZnO molecules (solid arrow) lead to the saturation of ZnO on the Au particle and subsequent formation of ZnO nuclei. Finally ZnO nanowires grow from nuclei. b) Lower flux of adsorbed ZnO molecules (dotted arrow) drives the energetically more favorable ZnO nucleus at the Au–ZnO nanowire interface. Open arrow: direct impingement. The nanowire grows in a layer-by-layer fashion through the reiterative building of successive ZnO layers with assistance of Au particle.

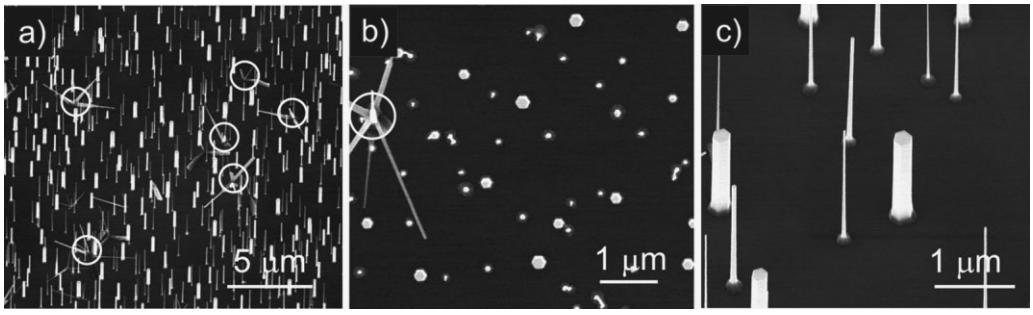

Figure 5. SEM images of epitaxially grown ZnO nanowires on a GaN/Si substrate. a) Low-magnification SEM image. The position of Au particles is marked by a circle. b) Top view of ZnO nanowire grown on a GaN/Si substrate. Hexagonal facets are clearly visible. c) Close view of vertically aligned ZnO nanowires. Nanowires show the developed base shape.

those used for the nonepitaxial growth of wires A on SiO_2/Si substrates was used for epitaxial growth of ZnO nanowires on GaN/Si substrates. As shown in Figure 5, ZnO nanowires are grown not only at the original position of Au particles but also in the surrounding of these positions. Note that this phenomenon was not observed for wires A grown on SiO_2/Si substrates. The phase-mode atomic force microscopy (AFM) image of GaN/Si substrate after deposition of Au particles, followed by annealing at 500 °C with pressure of 1 mbar for 30 min, shows small Au clusters with a height of a few nm near the original Au particles (see Figure S5 in the Supporting Information). The formation of a ZnO nucleus and subsequent nanowire growth at Au site might take place in a similar way as described previously for wires A. However, ZnO nanowires, which were formed by the assistance of small Au clusters, grew epitaxially as shown in Figure 5. The surface migration of Au atoms might initiate nanowires growth near the original Au particles and limit the position control of ZnO nanowires. In addition, one can see clearly the development of the base widening as result of the surface diffusion of vapor species.[24] The cross-section TEM images of vertically aligned nanowires shows a sharp ZnO/GaN interface without Au clusters (Figure S6 in the Supporting Information). Au clusters after supporting the formation of ZnO nuclei may leave the location owing to the high diffusion rate of Au atoms at high growth temperatures. Most probably small Au clusters react with the GaN layer chemically during wire growth.[25] Therefore, in this case the Au particle catalyzing the ZnO nanowire growth remains neither at the root nor the tip after extended nanowire growth periods.

In summary, we have investigated Au-assisted growth of ZnO nanowires and nanowire branches. We first put special emphasis on the interaction between Au and adsorbed ZnO molecules. A simple growth model suggests that competition between the saturation rate and nucleation rate of ZnO on the Au particle results in two different growth modes, leading either to the presence of the catalytic Au particle at the root or at the tip of the ZnO nanowires. For Au-catalyzed wire growth, the diameter of the nanowires did not match that of the Au particles. Finally, it was demonstrated that the surface migration of Au atoms on GaN/Si substrates limits position-controlled growth of ZnO nanowires.

Experimental Section

Commercially available Au colloids (BBI International) were used as catalyst. For growth of typical wires A and B, Au colloids with mean diameter of 52 nm and a concentration of about 4.5×10^9 particles mL^{-1} were used. To disperse Au nanoparticles at the SiO_2/Si (the thickness of SiO_2 is 100 nm) and GaN/Si substrates, a diluted Au colloid solution was dropped on the substrates and subsequently dried by blowing Ar gas for a few seconds. This method resulted in a random distribution of Au particles over the substrate. A typical scanning electron microscopy (SEM) image of dispersed 50 nm Au particles with an approximate density of 0.2 particles μm^{-2} on the substrate is given in the Supporting Information (Figure S1a). The Au colloid solution was diluted with ethanol. If water was used, no Au particles were deposited on the substrate. It was possible for the Au particles to attach to the substrate by van der Waals forces. Then, the sample was cleaned with O_2 plasma at a power of 150 W for 2 min, and then annealed at 500 °C for 30 min. O_2 plasma treatment was carried out with a pressure of 0.7 Torr (the base pressure was 0.2 Torr) and O_2 flow rate of 70 sccm at room temperature. This final step is important for the growth of nanowires because residual organic materials disturb the growth of nanowires. Note that the thin gold oxide shell formed on the nanoparticles after O_2 plasma will be thermally decomposed during the annealing process at 500 °C or at even higher growth temperatures.[26]

The growth experiments were carried out in a tube furnace integrated with Ar gas flowing and pumping systems.[12] ZnO and graphite powder with a ratio of 1:1 in wt % were used as source material. The tube pressure was maintained at 200 mbar under a constant Ar flow of 30 sccm for wire growth. Owing to the temperature gradient in the growth tube, the temperature at the source and the substrates where the nanowires were collected were 920 °C and 850 °C, respectively. The substrates were placed in 12 cm away from the source boat, which was located at the center of the heating zone.

ZnO nanowire branches were grown in a similar way. A diluted 50 nm Au colloid solution (4.5×10^9 particles mL) was dropped on the nanowires grown substrates and subsequently dried by blowing Ar gas. A typical SEM image of Au nanoparticles dispersed on the ZnO naonwires is shown in the Supporting Information

(Figure S1b). The sample was annealed at 500 °C for 30 min prior to the growth run, in which the same growth parameters were used as for the growth of wires A.

Keywords:
chemical vapor transport · crystal growth · nanowires · oxides · semiconductors

[1] C. Yang, Z. Zhong, C. M. Lieber, *Science* **2005**, *310*, 1304.
[2] M. T. Björk, B. J. Ohlsson, T. Sass, A. I. Persson, C. Thelander, M. H. Magnusson, K. Deppert, L. R. Wallenberg, L. Samuelson, *Appl. Phys. Lett.* **2002**, *80*, 1058.
[3] J. B. Hannon, S. Kodambaka, F. M. Ross, R. M. Tromp, *Nature* **2006**, *440*, 69.
[4] F. M. Ross, J. Tersoff, M. C. Reuter, *Phys. Rev. Lett.* **2005**, *95*, 146104.
[5] F. M. Kolb, H. Hofmeister, R. Scholz, M. Zacharias, U. Gösele, D. D. Ma, S. T. Lee, *J. Electrochem. Soc.* **2004**, *151*, G472.
[6] A. I. Persson, M. W. Larsson, S. Stenström, B. J. Ohlsson, L. Samuelson, L. R. Wallenberg, *Nat. Mater.* **2004**, *3*, 677.
[7] Y. Wang, V. Schmidt, S. Senz, U. Gösele, *Nat. Nanotechnol.* **2006**, *1*, 186.
[8] S. Kodambaka, J. Tersoff, M. C. Reuter, *Science* **2007**, *316*, 729.
[9] L. Schubert, P. Werner, N. D. Zakharov, G. Gerth, F. M. Kolb, L. Long, U. Gösele, *Appl. Phys. Lett.* **2004**, *84*, 4968.
[10] S. A. Dayeh, E. T. Yu, D. Wang, *Nano Lett.* **2007**, *7*, 2486.
[11] I. Levin, A. Davydov, B. Nikoobakht, N. Sanford, P. Mogilevsky, *Appl. Phys. Lett.* **2005**, *87*, 103110.
[12] D. S. Kim, R. Ji, H. J. Fan, F. Bertram, R. Scholz, R. Dadgar, K. Nielsch, A. Krost, J. Christen, U. Gösele, M. Zacharias, *Small* **2007**, *3*, 76.
[13] S. Helveg, C. López-Cartes, J. Sehested, P. L. Hansen, B. S. Clausen, J. R. Rostrup-Nielsen, F. Abild-Pedersen, J. K. Nørskov, *Nature* **2004**, *427*, 426.
[14] Y. Li, W. Kim, Y. Zhang, M. Rolandi, D. Wang, H. Dai, *J. Phys. Chem. B* **2001**, *105*, 11424.
[15] J. Gavillet, A. Loiseau, C. Journet, F. Willaime, F. Ducastelle, J.-C. Charlier, *Phys. Rev. Lett.* **2001**, *87*, 275504.
[16] K. Polacer, E. F. Wassermann, *Thin Solid Films* **1976**, *37*, 65.
[17] E. F. Wassermann, K. Polacek, *Appl. Phys. Lett.* **1970**, *16*, 259.
[18] M. H. Huang, Y. Wu, H. Feick, N. Tran, E. Weber, P. Yang, *Adv. Mater.* **2001**, *13*, 113.
[19] R. S. Wagner, W. C. Ellis, *Appl. Phys. Lett.* **1964**, *4*, 89.
[20] M. Kirkham, X. Wang, Z. L. Wang, R. L. Snyder, *Nanotechnology* **2007**, *18*, 365304.
[21] U. Pal, J. García-Serrano, G. Casarrubias-Segura, N. Koshizaki, T. Sasaki, S. Terahuchi, *Sol. Energy Mater. Sol. Cells* **2004**, *81*, 339.
[22] P. Buffat, J.-P. Borel, *Phys. Rev. A* **1976**, *13*, 2287.
[23] L. A. Lewis, A. M. Cameron, *Metal. Mater. Trans. B* **1995**, *26*, 911.
[24] Y. Kim, H. J. Joyce, Q. Gao, H. H. Tan, C. Jagadish, M. Paladugu, J. Zou, A. A. Suvorova, *Nano Lett.* **2006**, *6*, 599.
[25] A. Barinov, L. Casalis, L. Gregoratti, M. Kiskinova, *J. Phys. D: Appl. Phys.* **2001**, *34*, 279.
[26] L. K. Ono, B. Roldan Cuenya, *J. Phys. Chem. C.* **2008**, *112*, 4676.
[27] L. Cao, B. Garipcan, J. S. Atchison, C. Ni, B. Nabet, J. E. Spanier, *Nano Lett.* **2006**, *6*, 1852.

Received: January 4, 2008
Revised: April 7, 2008
Published online: September 3, 2008

